The geometry and evolution of magma pathways through migmatites of the Halls Creek Orogen, Western Australia

N. H. S. OLIVER

School of Applied Geology, Curtin University, GPO Box U1987, Perth, Australia, 6001

AND

T. D. BARR

Department of Earth Sciences, Monash University, Clayton, Victoria, Australia, 3168

Abstract

In the Halls Creek Orogen of north-western Australia, the distance of melt migration through migmatitic metasedimentary rocks and adjacent metabasites is partly constrained by relationships of leucosomes and small mafic magma veins to rock boundaries and structural elements. Stromatic leucosomes in metasediments are cut by a network of small extensional fractures and shear zones, oriented steeply during melt migration. These shear zones allowed cm- to 10 m-scale migration of felsic magma derived by *in situ* anatexis. In the adjacent metabasite layers, a similar shear array allowed injection of H_2O-undersaturated mafic to ultramafic magma, locally dehydrating and chemically modifying these rocks. However, these mafic to ultramafic veinlets are too mafic to be explained by *in situ* anatexis, necessitating an external magma source. Also, the lack of felsic veinlets cutting metabasites, and mafic veinlets cutting metasediments, requires that vertical inter-connectivity of these fracture systems was restricted. We propose along-layer migration of mafic to ultramafic magma through the metabasite, assisted by horizontal connection of the shear zones. This migration occurred independantly of metre-scale felsic magma migration in the adjacent metasediments, even though these two deformation-assisted magma migration systems may have been operating at the same time.

KEYWORDS: deformation, magma migration, anatexis, fracture, migmatite.

Introduction

THE migration of magma from source regions into granitoid plutons is of current interest, both with respect to the composition and chemical evolution of granitoids and the nature of the magma extraction and transport mechanisms (see reviews by Clemens, 1990; Brown, 1994). In order for magma to leave migmatite terrains and segregate into larger granitoid bodies, deformation is currently considered to play an important role, at least locally. Observations of the inter-relationship between deformation and anatexis, as observed in well exposed migmatite terrains, can lead to a better understanding of the magma—rock segregation process. Here, we document the config-uration of various leucosomes and dykes in part of the Halls Creek Orogen, and use their inter-relations with the different rock types and structures to attempt to ascertain over what scale magma pathway interconnection occurred, and how far magma moved in these pathways.

Local geology

The Halls Creek Orogenic Belt of northwestern Australia forms part of an L-shaped zone of Proterozoic rocks (Fig. 1) that Tyler *et al.* (1994) propose is part of an 1870 to 1800 Ma collisional orogen. Key migmatite outcrops surround water holes in the rocky bed of Fletcher Creek, approximately 5 km north of the Sally Malay Ni-Cu prospect, in the amphibolite-granulite facies 'Tickalara Metamorphics'
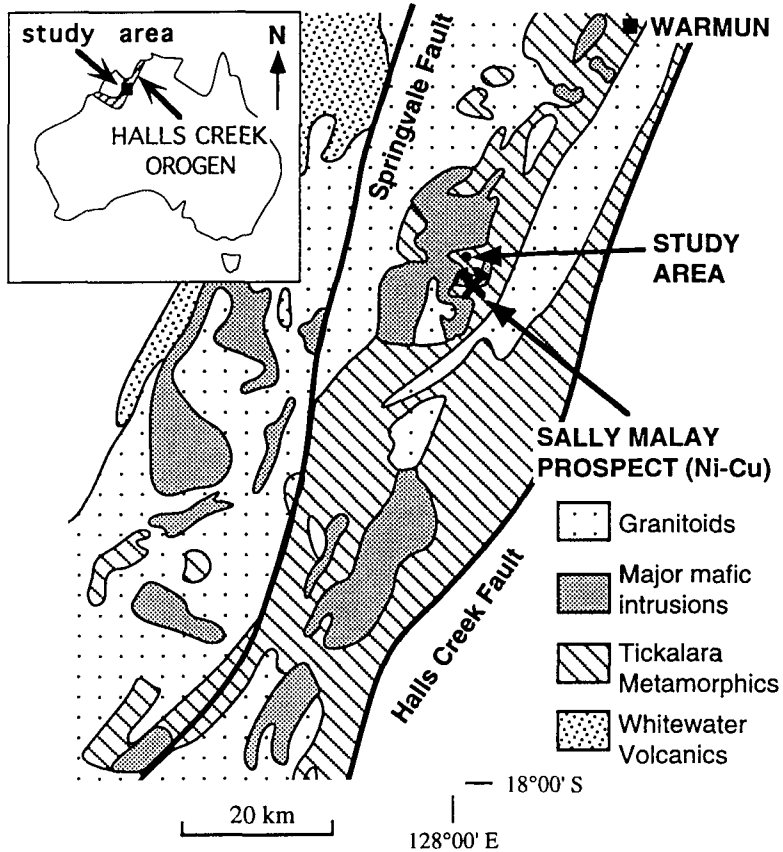
FIG. 1. Map showing the central amphibolite- to granulite facies part of the Halls Creek Orogen, modified from Blake and Hoatson (1993).

(Fig. 1). Mafic, felsic, pelitic and psammopelitic rocks were metamorphosed to maximum T–P conditions of 750 to 800°C at 3.5 to 4.5 kbar (Thornett, 1986) although temperatures may locally have exceeded this in the vicinity of mafic intrusions (see below). Voluminous pre-, syn- and post-metamorphic intrusions comprise >80% of the outcrop area regionally, and include substantial parts of the Tickalara Metamorphics as well as mapped plutons (Fig. 1). The intrusions include approximately equal proportions of gabbro and granite and the outcrop studied is part of a kilometre-scale roof pendant of a composite late-tectonic gabbro-granite body (Thornett, 1986). Extrapolation of the available U-Pb zircon geochronology suggests intrusion of most of these rocks occurred in the range 1850 to 1830 Ma (Page and Sun 1994) broadly synchronous with the metamorphic peak around 1850 Ma (Page and Hancock 1988).

The strongest deformation event formed a regionally distributed granoblastic to gneissic foliation (S_1) in mafic and pelitic rocks that was near-horizontal in the Sally Malay area prior to later deformation (Thornett, 1986). This fabric is defined in metapelitic gneisses by strong alignment of spinel- and cordierite-bearing mesosomes and garnet- and cordierite-bearing leucosomes, and in metabasites by aligned hornblende, plagioclase and some pyroxene. Low-pressure, lower granulite facies conditions were thus reached during this penetrative deformation. Inferred F_2 recumbent folds are present at regional scales, with S_2 parallel to S_1 except in rare F_2 fold hinges (Thornett, 1986). The rocks and the S_1 fabric are folded by kilometre-scale shallow-plunging east-west trending F_3 folds (Fig. 2). The absolute timing of these fabrics is as yet only loosely constrained by the available geochronological data.
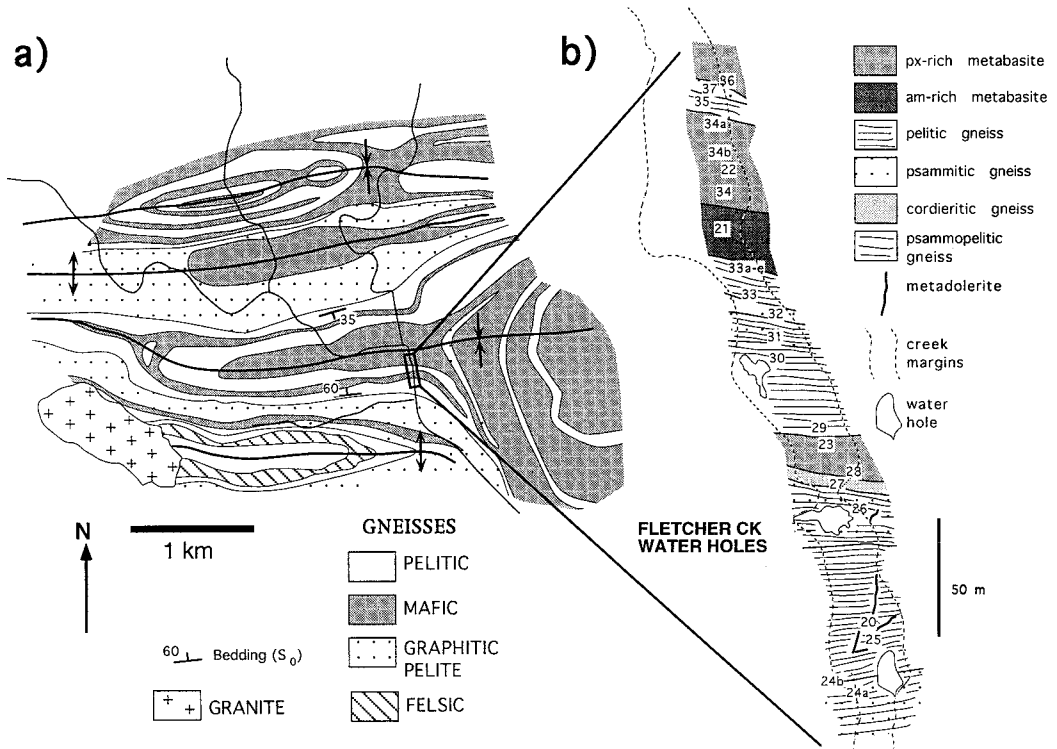
FIG. 2. (a) Macro-scale geology of the upper reaches of Fletcher Creek, showing the distribution of the major rock units, folded around open F_3 folds. Based on mapping by Thornett (1986), regional reconnaissance and air photograph interpretation by the authors, and detailed mapping in the small area indicated. (b) Outcrop-scale geological map of the exposed bed of Fletcher Creek ('Fletcher Creek water holes'), for the area shown in (a). Numbers shown correspond to our major sampling and observation sites.

Field relations

The geometry of the different rocks at Fletcher Creek provides evidence for the relative timing of events and the nature of magma–wallrock interaction. Boundaries between most rock types are parallel to the well developed foliation (S_1, Fig. 2). Metasedimentary rocks can be subdivided at a range of scales, with fairly continuous units being preserved that are presently as little as 0.02 to 1 m thick. The latter are traceable at the 5 to 10 m-scale within the creek outcrops, and 5 to 100 m-thick units can be followed over several kilometres (Fig. 2). Although the rocks are strongly deformed in hand-specimen the map-scale units do not appear to have been transposed and an approximate stratigraphic column could be constructed from the map pattern shown in Fig. 2. Centimetre- to m-scale shear zones, magmatic and subsolidus veins, and rounded to kink-like minor folds overprint the penetrative S_1 foliation,

and are the key features of interest in this study. The later F_3 folding does not develop a penetrative foliation. Local meso-scale F_3 folds in the hinge of the main east–west trending macroscopic F_3 fold (Fig. 2) overprint most of the anatectic features decribed in these outcrops.

Stromatic migmatite in metasediments. Syn-D_1 migmatites are predominantly stromatic and meta-texitic, with 2–20 mm wide leucosomes parallel to S_1 (Fig. 4). Grain sizes are characteristically coarser in the leucosomes (up to 1 mm) than the surrounds (average 0.2 mm). These migmatites contain (1) paleosomes of microcline, plagioclase, biotite, cordierite ± quartz ± spinel ± sillimanite; (2) melanosomes of biotite, cordierite, plagioclase, spinel ± sillimanite ± quartz; and (3) leucosomes of quartz, biotite, plagioclase, garnet, microcline, cordierite ± plagioclase ± sillimanite.

In the paleosomes and melanosomes, sillimanite and spinel are armoured by cordierite. In the

leucosomes, garnet, quartz and feldspars show smooth grain boundaries, with quartz commonly embayed by garnet. Cordierite in leucosomes is commonly free of inclusions and alteration products, but is also locally retrogressed to andalusite + muscovite, and/or andalusite + biotite + quartz ± sillimanite, the latter assemblage commonly as symplectites.

These assemblages and the field relations are consistent with generation of *in situ* partial melt during low-pressure granulite facies metamorphism, synchronous with D_1 deformation. Based on the textural relations, the prograde path is inferred to involve the breakdown of sillimanite and spinel at the expense of cordierite, and partial melting reactions that produced cordierite and garnet. Similar prograde relations were observed by Vernon *et al.* (1990), although at slightly lower pressures and with andalusite as the aluminosilicate.

Psammopelitic layers interbedded with the metapelites contain similar foliation-parallel leucosomes, although in lesser abundance than the pelites, and with quartz present and spinel absent. The most psammitic layers contain the least foliation-parallel leucosomes. These relationships may be due to mechanical contrasts between the layers permitting different amounts of magma access, but more likely reflect a bulk compositional control on the amount of magma produced and frozen *in situ* (e.g. Clemens and Vielzeuf, 1987; Johannes and Holtz, 1990). Also, in contrast to the other leucosome types (see below), there is little variation in the distribution and percentage of garnet relative to quartz and feldspar in foliation-parallel leucosomes of a given metasedimentary layer. This could reflect little kinetic hindrance to garnet growth in these magmas (e.g. Powell and Downes, 1990), but may also be a result of little separation of the solid and liquid products of the melting reactions, suggesting limited movement of magma from the site of production which might otherwise segregate melt and crystals (cf. Ellis and Obata, 1992; Brown, 1994; Brown *et al.*, 1995).

Vein-type migmatite. The second type of migmatite is associated with veins and boudin-necks, and consistently cuts the stromatic migmatite. It occurs as cm-scale veins or blebs rarely up to 0.5 m across (Figs 3, 4*a*), and irregularly crossing vein networks resulting in local diatexitic migmatite (Fig. 4*b*). The more regular leucosome veins are typically steep, striking 020° to 060°, and mostly show sinistral shear displacement across their boundaries, although conjugate veins with dextral offset are also locally present (Figs 3, 5). The boudin-neck vein-type leucosomes appear both symmetrically and asymmetrically distributed around boudin ends.

The leucosomes contain coarse-grained quartz, K-feldspar, biotite, cordierite, garnet ± plagioclase.

The garnets are irregularly distributed and rounded, commonly rimmed by biotite ± cordierite. They may reach grain sizes up to 2 cm in diameter, and typically occur in clusters within the thickest parts of these veins (Fig. 4*a*), leaving other parts of the veins garnet-poor. The leucosomes commonly crosscut pelite/psammite boundaries, and, rarely, metasediment/metabasite boundaries (Fig. 5). They are nearly as abundant within psammitic layers as they are in pelitic layers. These observations suggest that the melts have migrated from a melt-generation site to their current position over distances of a few cm to a few m, the range of widths of layers that are cut by these leucosomes (Figs 3, 5).

Kinematically, the data are consistent with anatexis and leucosome segregation during layer-normal shortening and layer-parallel (to slightly oblique) extension (Fig. 5), as has also been observed elsewhere by Wickham (1987), Sawyer (1991), and Brown *et al.* (1995), amongst others.

Mafic dykes and surrounding felsic leucosomes. Mafic dykes 0.2 to 2 m wide, dissimilar in appearance to strongly foliated S_1-parallel metabasites (see below), mainly cut the S_1 gneissosity at a high angle (Fig. 3). The dykes contain hornblende, plagioclase, cummingtonite, biotite, and orthopyroxene, the latter two minerals dominating the margins. This assemblage suggests crystallization temperatures in excess of 1000°C, well above the solidus of the surrounding pelites. The presence of primary igneous hornblende, with metamorphic porphyroblasts of orthopyroxene growing in the dyke margins, suggests emplacement at or soon after the metamorphic peak, in contrast to the earlier metabasites that contain only metamorphic minerals and are well foliated. The margins may be weakly foliated (mainly biotite) parallel to the gneissosity in the surrounding pelites, indicating they have undergone some north–south shortening. These dykes also show convoluted, bulbous boundaries (Figs 3, 4*d*).

The boundary between the dykes and the pelitic wallrocks is commonly obscured by the presence of microgranite representing the third migmatite type. The granite sheaths the mafic dykes, forming (*a*) diffusely-bounded diatexitic migmatite containing xenoliths of pelite and mafic dyke (Figs 3, 4*d*); grading into (*b*) discrete dykes of microgranite with abundant garnet-cordierite clots to 1 cm across (Fig. 3, near bottom); and (*c*) 'back-veins' within the mafic dykes (Figs 3, 4*c*), where biotite-rich reaction zones are produced in the mafic rock. Although there is a wide variation in mafic dyke and felsic sheath widths, the width of the felsic sheath is approximately proportional to the width of the mafic dyke. The felsic magma contains comparatively fine grained quartz, plagioclase biotite, cordierite ± garnet ± K-feldspar. It post-dates the
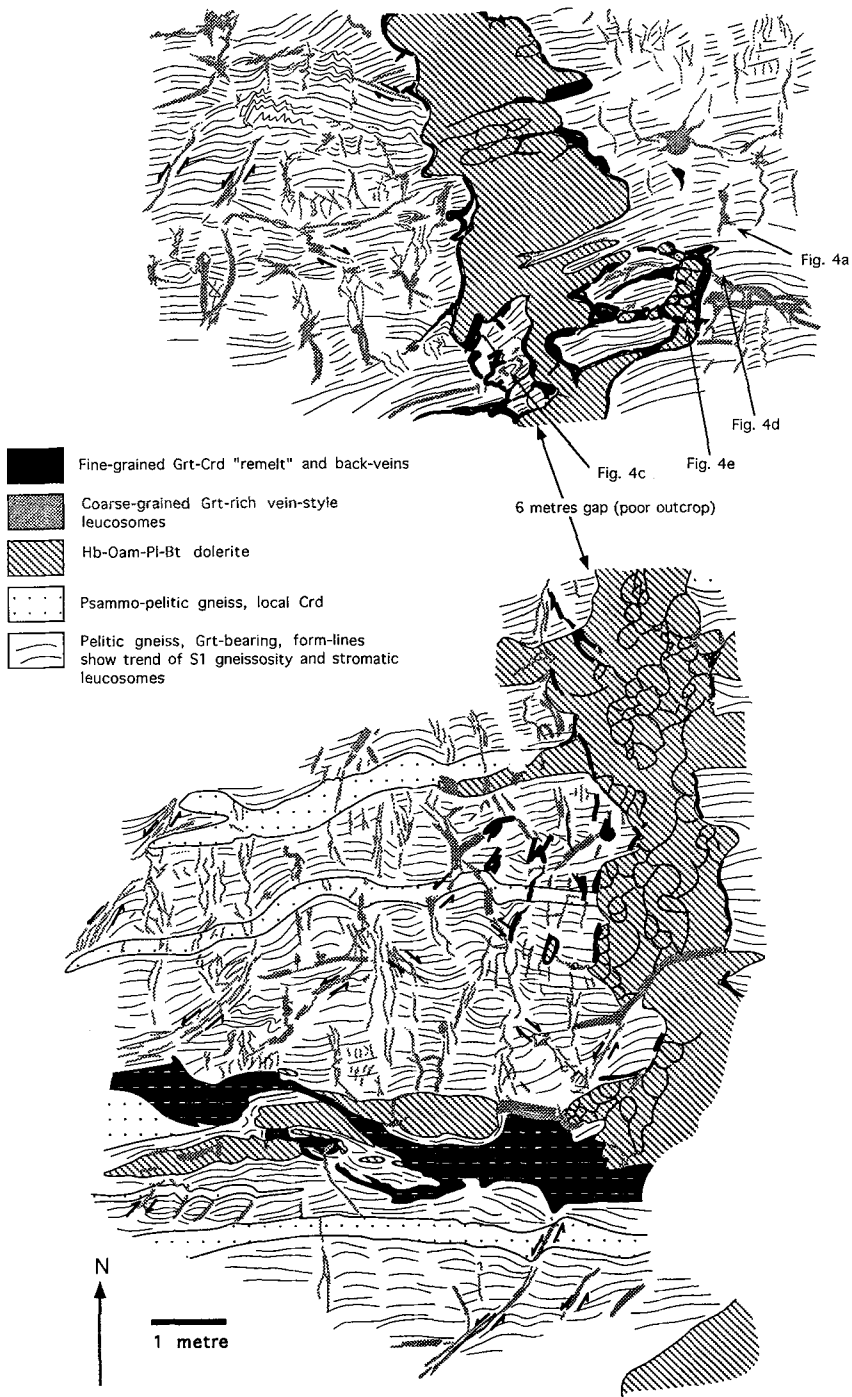
Fig. 4a

Fig. 4d

Fig. 4c

Fig. 4e

6 metres gap (poor outcrop)

Fine-grained Grt-Crd "remelt" and back-veins

Coarse-grained Grt-rich vein-style leucosomes

Hb-Oam-Pl-Bt dolerite

Psammo-pelitic gneiss, local Crd

Pelitic gneiss, Grt-bearing, form-lines show trend of S1 gneissosity and stromatic leucosomes
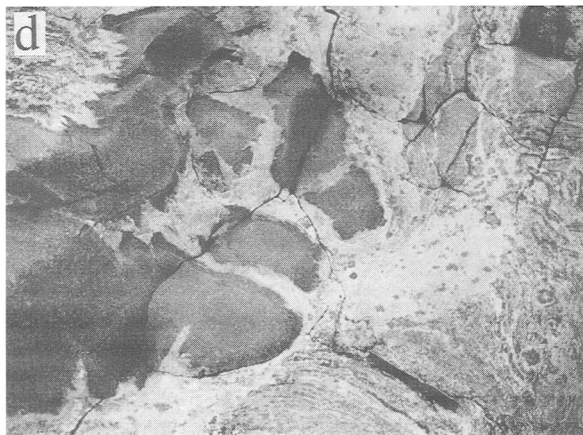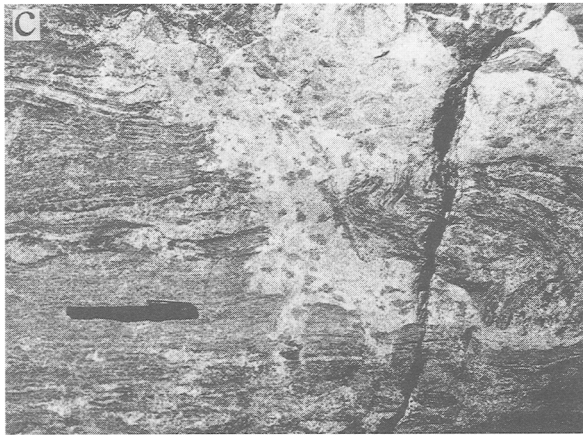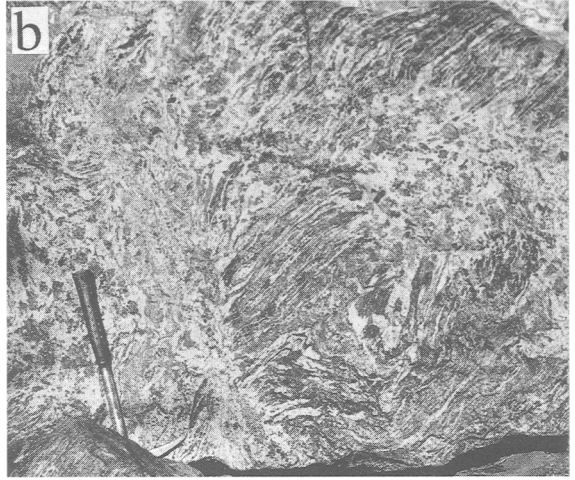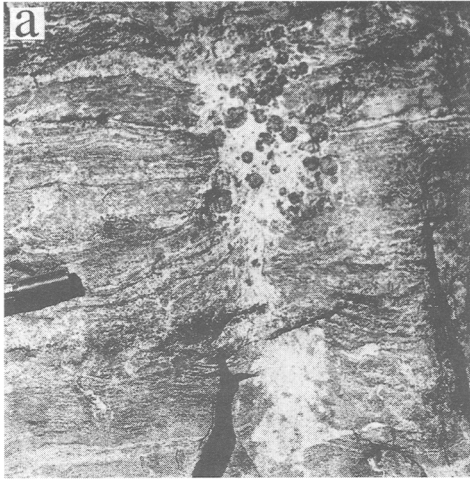
N

1 metre

FIG. 3. Detailed outcrop geological map of locations 20 (upper sketch) and 25 (lower sketch) on Fig. 2b, constructed using grid mapping at 1:50 scale, showing the inter-relationships between the different migmatite types, crosscutting mafic dykes, and fabric elements referred to in the text.
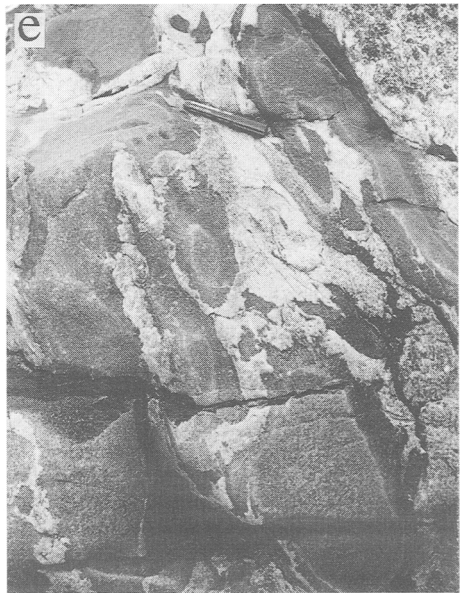
formation of the stromatic migmatites (Fig. 4c, d) and is broadly synchronous with the vein-type migmatite as suggested by localization of some of the melt in similar veins and boudins (Fig. 3).

These observations suggest that (a) dyke intrusion, and formation of the sheath, occurred during deformation; (b) dykes were emplaced into already hot rocks, causing anatexis around their margins; and (c) the surrounding rocks may have been already partially molten at the time of dyke emplacement. Simplified 1-D thermal modelling of the emplacement of 10cm wide mafic dykes (the narrowest observed) at 1000 to 1100°C reveals that the wallrock temperatures must have exceeded 450 to 600°C to produce 1 to 5 cm wide anatectic felsic sheaths, assuming anatexis commenced at 750°C (Fig. 6). Calculations for 1 to 2m wide dykes producing 10 to 50 cm wide sheaths (e.g. Fig. 4d) give similar results. Although there are many assumptions made in the models, the results broadly support the field observations.

Metabasites with crosscutting pyroxene veins. Metabasites form 10 cm to 50 m wide bands, parallel to bedding in the metasediments, that represent former flows or sills. Boundaries between some of the different metabasites (Fig. 2) are defined by distinctive colour changes, variations in the hornblende/pyroxene ratio, and corresponding variation in their whole-rock geochemistry (Fig. 7). With respect to igneous precursors, amphibole-rich metabasites are not cogenetic with pyroxene-rich metabasites with which they are locally in contact, nor with the cross-cutting (and locally layer-parallel) metadolerite dykes (Fig. 7). This is important in attempting to define the origins of the younger mafic dykes and veinlets (see discussion). Amphibole and plagioclase in both the amphibole-rich and pyroxene-rich metabasites define S_1. Pyroxene in the pyroxene-rich metabasites is porphyroblastic and is weakly aligned in this fabric, but also locally cross-cuts it.

Vein-like pyroxene-rich zones, 0.5 to 4 cm wide, overprint the above granoblastic- to aligned assemblages. Most veins are oriented steeply, striking 025 to 057°, similar to the orientation of the vein-type migmatite described in the pelites. The first variety of this type forms a distinctive array of cm-scale discontinuous replacement veins (location 23 Fig. 2), containing coarse-grained (up to 0.8 cm) poikilitic orthopyroxene + clinopyroxene ± plagioclase (Fig. 8a). In thin-section, the pyroxene overgrows the S_1 foliation without significantly disrupting it, indicating it has grown under subsolidus conditions. Rarely, the veins contain thin cores of non-poikilitic pyroxene that may represent material precipitated directly from a fluid or melt in a fracture. Approximately constant volume comparison of vein-bearing with vein-absent rocks with similar Si/Al ratios shows that introduction of the pyroxene resulted in an enrichment of S and Cu, a probable increase in the Fe^{2+}/Fe^{3+} ratio (based on the negative loss-on-ignition in the vein-rich rocks), an inferred decrease of H_2O and decreases in K, Cl, Zn, and Ba (Fig. 8b). These metasomatic changes and the textural observations are consistent with the production of two pyroxenes by breakdown of amphibole, in the presence of a fracture-hosted fluid or melt that was initially out of equilibrium with the wallrocks. Closure of the fractures may have ejected the bulk of the melt or fluid, leaving narrow dehydration zones (now represented by the bulk of the replacement veins) as evidence.

The second type occurs as 0.5 to 2 cm-wide pyroxene-rich rims surrounding orthopyroxene + hornblende ± clinopyroxene ± plaoioclase ± orthoamphibole norite and pyroxenite dykelets of similar width (location 21, Fig. 2). The pyroxene-rich rims are mineralogically similar to the replacement veins described above, suggesting a common origin, the main difference being the different degree of preservation of the frozen magma in the core of the veins (Fig. 9).

Discussion

Metasediments. Anatexis associated with shear zones presents a 'chicken-and-egg' problem whereby initiation of one could lead to development of the other, but outcrop patterns do not always allow distinction. In the vein-style migmatites here, melting may have been triggered in dilatant shear fractures,

FIG. 4. Migmatite types in metasedimentary gneisses from the Fletcher Creek water holes, mainly from locations 20 and 25 (Figs. 2, 3). Pen for scale except where indicated. (a) Vein-type migmatite, here localized in a zone of symmetric boudinage of the S_1 fabric and stromatic migmatites. Note the diffuse contact between the vein-type leucosome and the stromatic migmatite, the coarse rounded garnet grains, and the irregular distribution of the garnet grains within the leucosome; (b) Vein-type migmatite coalescing into diatexitic migmatite, in pelitic gneiss. 40 cm hammer for scale; (c) S_1-parallel stromatic migmatite (left), folded by possible F_2 folds (right), and cut by fine-grained discordant leucosomes with clots of garnet ± cordierite - biotite; (d) Mafic (metadolerite) dyke cutting metapelitic gneisses with stromatic migmatite, and sheathed by fine-grained discordant leucosome; (e) Mafic dyke, sheathed by discordant leucosome generated by intrusion of the dyke into hot wallrocks, which has back-veined into the dyke, producing cm-scale reaction rims rich in biotite (dark).
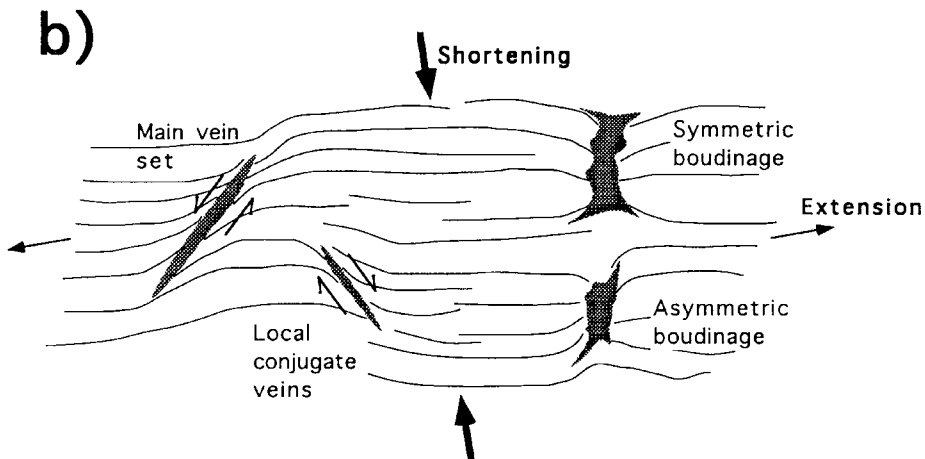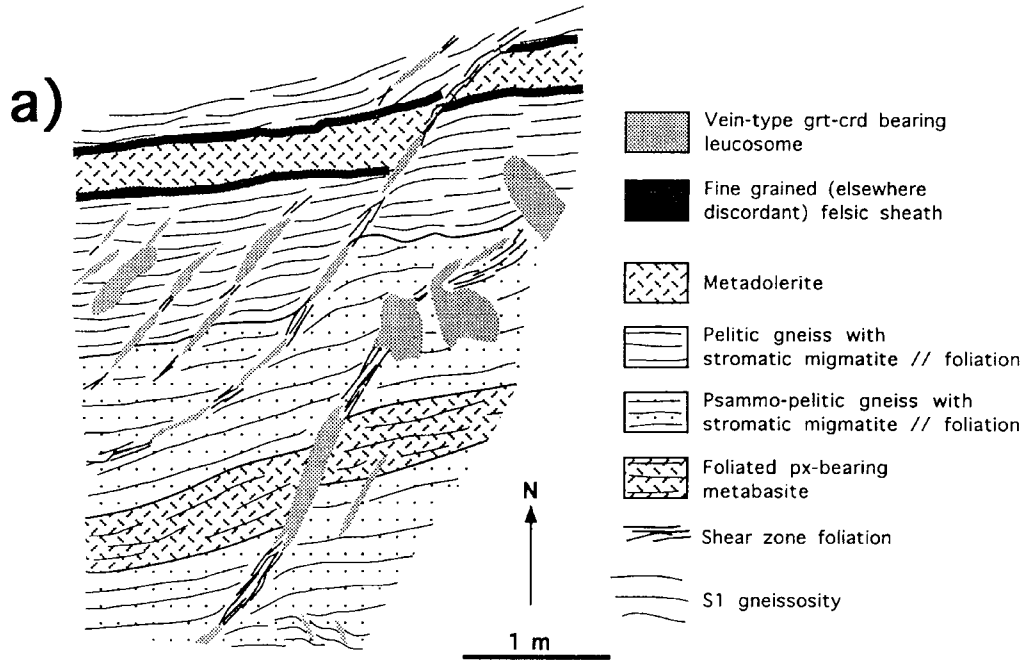
FIG. 5. (a) Detailed outcrop sketch from location 24b (Fig. 2), at a major contact between psammopelitic and pelitic gneisses, showing relative timing relationships between the three leucosome types, and the association of the vein-type leusosomes with S₁-transgressive shear zones. Note the variable proportion of leucosome along and around the shear zones; (b) Schematic geometry of vein-type leucosomes observed in metasediments of the Fletcher Creek water holes, their association with shear zones and boudinage, and the inferred approximate directions of shortening and extension.
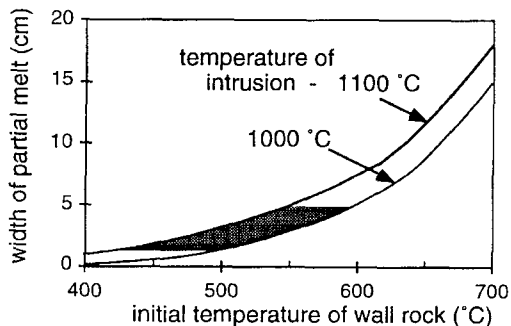
FIG. 6. Results of one-dimensional finite difference modelling to calculate the width of rock elevated above anatectic temperatures surrounding dykes 10 cm wide (after Price and Slack, 1954). Model conditions include an initially isothermal host rock, anatexis commencing at 750°C by biotite breakdown, and a latent heat of 300 J/g for both the fusing metapelites and the crystallizing mafic dyke (Jaeger, 1964). Shaded area indicates minimum temperatures calculated from observed widths of microgranitoid sheaths around the thinnest dykes in the outcrops.
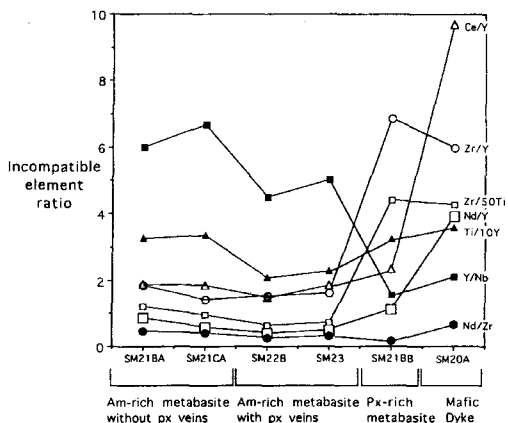

FIG. 7. Geochemistry of mafic rocks from the Fletcher Creek water holes, expressed as incompatible element ratios. The first five samples are from the foliated metabasites, the first four of which show sufficient colinearity in these data that we infer a common parent magma. The pyroxene-rich metabasite, and the younger cross-cutting metadolerite, appear unrelated to the amphibolites.

by stress drops associated with fracture formation, and these underpressured molten veins may then become sites towards which further melt would migrate until magma pressure increases again (see also Sawyer 1994; Brown *et al.*, 1995). Migration of aqueous fluid under sub-solidus conditions by such dilatancy pumping has been proposed by many authors (e.g. Etheridge *et al.*, 1983; see review by Oliver, 1996). Alternately, deformation of rock containing two irregularly distributed materials of
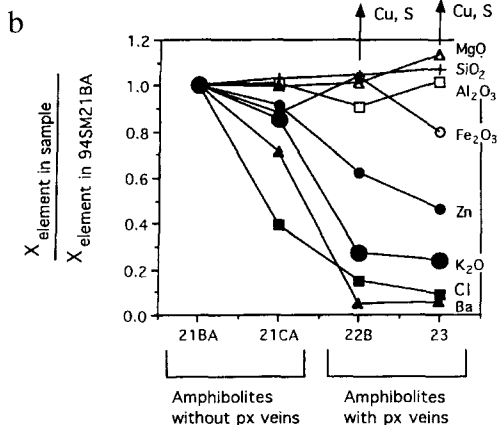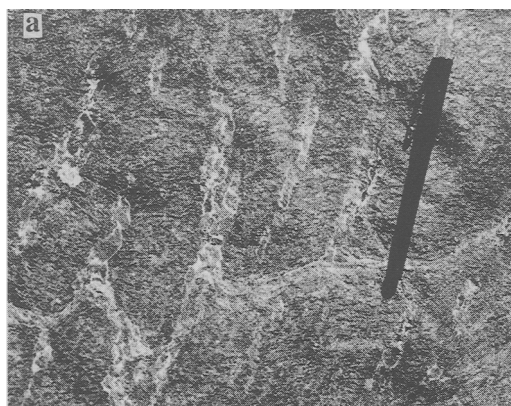

FIG. 8. (*a*) Replacement veins of 2 pyroxenes-plagioclase cutting foliated amphibolite, caused by passage of water-poor melt in thin fractures. (*b*) Geochemical comparison of amphibolitic metabasites, showing the effects of the pyroxene veins on the geochemistry of inferred similar precursor rocks (Fig. 7). 21BA is taken as the reference material as it has the least pyroxene veining — the other samples show a progressive increase in veining, to a maximum represented by Fig. 8*a*. Large volumes of sample (approx. 10 kg each) were prepared in order to obtain representative vein densities.

FIG. 9. Contact between two metabasites, cut by a brittle-ductile shear zone cored by a pyroxene-rich vein. In the amphibole-rich metabasite (top), the passage of melt is expressed by a noritic vein, inferred to have crystallized from a melt, and a narrow surrounding rim in which orthopyroxene is developed. In the pyroxene-rich metabasite (bottom), the inferred passage of the same melt is expressed as a dehydration zone (all amphibole removed) without a visible fracture, indicating a genetic link between intrusion of mafic to ultramafic melts and the pyroxene-rich replacement veins observed nearby (Fig. 8).

strongly contrasting rheology (such as wallrock with dispersed melt patches) will typically result in elongation of the soft materials into shear zones because of the viscosity contrast (e.g. Ross *et al.*, 1987; Bons and Urai, 1994). The range of leucosome-wallrock patterns observed can provide some answers to this problem (Fig. 5). Symmetric and asymmetric boudinage structures most likely reflect a cycle of ductile necking and stress increase, followed by pumping of melt towards boudin-forming fractures accompanying stress drop (see also van der Molen, 1985). However, the ductile shear zones are proportionally longer in one direction than the asymmetric boudinage structures; they cut several rock layers, and do not generally appear to have the dilatant jog geometries that would perhaps be expected if all the melt had pooled in these shear zones by dilatancy pumping. Bending and narrowing of the S_t foliation in the outer parts of these shear zones requires that strain was accumulated primarily in the solid state, according to the conventionally accepted model of formation of ductile shear zones (Ramsay, 1980), even if the presence of melt enhanced such deformation by reduction of shear stresses. The present distribution of leucosomes in and around shear zones (e.g. Fig. 5a) probably

reflects the combined effects of (1) initiating shear in partially molten rocks, (2) propagation of shear zones along distributed sites of melting, (3) migration of the melt along the shear zone as shear strains accumulate, and (4) both pooling and local expulsion of the magma as shearing ceases, resulting in individual shear zones with melt-poor and melt-rich portions. Magma pressure and behaviour during such a complicated cycle will be quite variable, and may not correspond in any clear way to overpressure/underpressure cycling expected for simple dilatancy pumping.

Metabasites. The pyroxene-rich veins cutting the metabasites have similar geometry, shear-sense and boudinage patterns to the vein-style leucosomes in the metasediments, suggesting that they were formed under similar kinematic conditions, and possibly at the same time. However, although *in situ* anatexis produced abundant leucosomes in metapelites, mafic to ultramafic magma in the fractures cutting metabasites must have been sourced externally. These quartz-absent host rocks cannot have undergone anatexis under lower granulite facies conditions (Rushmer, 1991). If temperatures had been higher than suggested by thermobarometry (Thornett, 1986) in the pelites (e.g. adjacent to the metadolerite dykes), any *in situ* melt produced would be trondhjemitic or tonalitic in composition (e.g. Peacock *et al.*, 1994). We recognise a range of pyroxene-bearing veins in these rocks similar to those observed by Pattison (1991), ranging from injected magmatic veins through to subsolidus replacement veins and rims.

Relationships between melt migration in metasediments and metabasites. The key observations regarding broader-scale melt migration in these outcrops are:

(1) vein-style leucosomes in the metasediments show no trace of having cut through the larger metabasite units shown on Fig. 2, although they do cut decimetre-scale metabasites (Fig. 5);

(2) the present distribution and geometry of vein-style leucosomes (and garnets within them) in metasediments reflects felsic magma migration over distances of up to several metres;

(3) there is no evidence that the narrow mafic veins cutting the metabasites have cut the metasediments; and

(4) the chemistry of the mafic veins cutting the metabasites requires that these veins were produced by interaction of the rocks with externally derived mafic to ultramafic magma that migrated at a scale broader than that of the outcrops studied (i.e. >100 m scale).

Buoyancy, compaction and deformation have the potential to influence magma extraction from migmatite terrains (e.g. Brown *et al.*, 1995). In

these outcrops, deformation appears to dominate m-to 10 m-scale magma flow. The rock layers were approximately horizontal at the time of D_1 deformation and anatexis. Our observations suggest that there was no vertical interconnection of the narrow mafic and felsic magmas during D_1, and hence that buoyancy and/or magma overpressure were insufficient to drive these magmas upwards for distances greater than 10 or 20 metres before they froze. Although we have not observed pooling of felsic magma underneath the overlying metabasites, nor of mafic magma underneath the overlying metasediments, the biggest felsic magma vein observed (Fig. 3) has not apparently been strongly influenced by an upwards driving force due to magma buoyancy. Rather, its orientation and thickness suggest deformation- or anisotropy-related migration and pooling of magma along the S_1 foliation, perhaps in a similar way as described previously for felsic magmas in the smaller shear-hosted veins. However, the presence of the externally derived mafic veins cutting the metabasites requires a significant distance of magma flow. These thin mafic veins are not related to the larger mafic dykes at the Fletcher Creek outcrops (Fig. 7), but share mineralogical and temporal similarities to large norite intrusions several kilometres to the east around Sally Malay (Fig. 1). Either the presently observed mafic veins have migrated across the metasedimentary layers exposed at Fletcher Creek without leaving an identifiable trace, or else magma migration was horizontal and layer-parallel. In the latter case, the shear zones observed in the metabasite layers may have provided the necessary plumbing system for long-distance flow of mafic magma. Magma flow systems in the two rock types have behaved independently, even though their geometry and relative timing relations raise the possibility that they may have been operating simultaneously.

Acknowledgements

References

Blake, D.H. and Hoatson, D.M. (1993) Granite, gabbro and migmatite field relationships in the Proterozoic Lamboo Complex of the East Kimberley region, Western Australia. *AGSO Journal of Australian Geology and Geophysics*, **14**, 319–30.

Bons, P.D. and Urai, J.L. (1994) Experimental deformation of two-phase rock analogues. *Materials Sci. Eng.*, **A175**, 221–9.

Brown, M. (1994) The generation, segregation, ascent and emplacement of granite magma: the migmatite-to-crustally-derived granite connection in thickened orogens. *Earth Sci. Rev.*, **36**, 83–130.

Brown, M., Averkin, Y.A., McLellan, E.L. and Sawyer, E.W. (1995) Melt segregation in migmatites. *J. Geophys. Res.*, **100**, 15655–79.

Clemens, J.D. and Vielzeuf, D. (1987) Constraints on melting and magma production in the crust. *Earth. Planet. Sci. Lett.*, **86**, 287–306.

Clemens, J.D. (1990) The granulite-granite connection. In: *Granulites and Crustal Evolution*. (D. Vielzeuf. and P. Vidal, eds.) Dordrecht, Kluwer Academic Publishers, **311**, 25–36.

Ellis, D.J. and Obata, M. (1992) Migmatite and melt segregation at Cooma, New South Wales. *Trans. Roy. Soc. Edinburgh*, **83**, 95–106.

Etheridge, M.A., Wall, V.J. and Vernon. (1983) The role of the fluid phase during regional metamorphism and deformation. *J. Metamorph. Geol.*, **1**. 205–26.

Jaeger, J.C. (1964) Thermal effects of intrusions. *Rev. Geophys.*, **2**, 443–66.

Johannes, W. and Holtz, F. (1990) Formation and composition of H_2O-undersaturated granitic melts. In *High-temperature Metamorphism and Crustal Anatexis*. (J.R. Ashworth and M. Brown, eds.) London, Allen and Unwin, 87–104.

Oliver, N.H.S. (1996) A review and classification of structural controls on fluid flow during regional metamorphism. *J. Metamorph. Geol.*, **14**, 477–92.

Page, R.W. and Hancock, S.L. (1988) Geochronology of a rapid 1.85–1.86 Ga tectonic transition: Halls Creek orogen, northern Australia. *Precambrian Res.*, **40/41**, 447–67.

Page, R.W. and Sun, S. (1994) Evolution of the Kimberley region, W. A. and adjacent Proterozoic Inliers — new geochronological constraints. *Geol. Soc. Austral. Abstr.*, **37**, 332–3.

Pattison, D.R.M. (1991) Infiltration-driven dehydration and anatexis in granulite facies metagabbro, Grenville Province, Ontario, Canada. *J. Metamorph. Geol.*, **9**, 315–32.

Peacock, S.M., Rushmer, T. and Thompson, A.B. (1994) Partial melting of subducting oceanic crust. *Earth. Planet. Sci. Lett.*, **121**, 227–43.

Powell, R. and Downes, J. (1990) Garnet prophyroblast-bearing leucosomes in metapelites: mechanisms, phase diagrams, and an example from Broken Hill, Australia. In *High-temperature Metamorphism and Crustal Anatexis*. (J.R. Ashworth and M. Brown, eds.) London, Unwin Hyman, 105–23.

Price, P.H. and Slack, M.R. (1954) The effect of latent

heat on numerical solutions of the heat flow equation. *Brit. J. Appl. Phys.*, **5**, 285–7.

Ramsay, J.G. (1980) Shear zone geometry: a review. *J. Struct. Geol.*, **2**, 83–99.

Ross, J.H., Bauer, S.J. and Hansen, F.D. (1987) Textural evolution of synthetic anhydrite-halite mylonites. *Tectonophys.*, **140**, 307–26.

Rushmer, T. (1991) Partial melting of two amphibolites: Contrasting experimental results under fluid-absent conditions. *Contrib. Mineral. Petrol.*, **107**, 41–59.

Sawyer, E.W. (1991) Disequilibrium melting and the rate of melt–residuum separation during migmatization of mafic rocks from the Grenville Front, Quebec. *J. Petrol.*, **32**, 701–38.

Sawyer, E.W. (1994) Melt segregation in the continental crust. *Geology*, **22**, 1019–22.

Thornett, J.R. (1986) *Evolution of a high-grade metamorphic terrain in the Proterozoic Halls Creek Mobile Zone, Western Australia.* University of Western Australia, PhD Thesis (unpubl.).

Tyler, I.M., Griffin, T.J., Page, R.W. and Shaw, R.D. (1994) The Halls Creek Fault System: repeated reactivation of a major tectonic boundary within the north Australian craton. *Geol. Soc. Austral. Abstr.*, **36**, 167–8.

van der Molen, I. (1985) Interlayer material transport during layer-normal shortening. Part II. Boudinage, pinch-and-swell and migmatite at Søndre Strømfjord Airport, west Greenland. *Tectonophys.*, **115**, 297–313.

Vernon, R.H., Clarke, G.L. and Collins, W.J. (1990) Local, mid-crustal granulite facies metamorphism and melting: an example in the Mount Stafford area, central Australia. In *High-temperature Metamorphism and Crustal Anatexis.* (J.R. Ashworth and M. Brown, eds.) London, Unwin Hyman, 272–319.

Wickham, S. (1987) Crustal anatexis and granite petrogenesis during low-pressure regional metamorphism: the Trois Signeurs Massif, Pyrenees, France. *J. Petrol.*, **28**, 127–69.